

Detection, Utilization and Avoidance of Nonlinear Dynamical Effects in Engineering Applications
Final Report of a Joint Research Project Sponsored by the German Federal Ministry of Education and
Research. 2001, Shaker Verlag, Aachen. pp.197-225.

Brake Squeal

K. Popp and M. Rudolph

Institut für Mechanik, Universität Hannover, Germany

Abstract

Due to increasing interest of car customers in comfort features, brake noise has become a major concern to brake suppliers. Noise showing frequencies above 1 kHz and a narrow bandwidth is usually called 'brake squeal'.

After a short introduction into squeal excitation mechanisms, a rigid body brake model displaying the main features of a floating caliper disc brake is presented.

A brake noise test rig has been installed and is used to verify model calculations which are based on the 14 DOF multibody system .

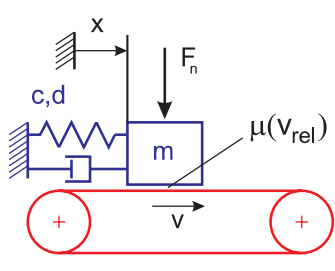
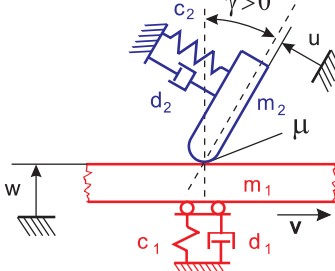
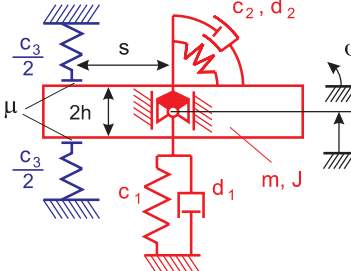
A stability analysis as well as an sensitivity analysis have been conducted in order to find recommendations for a brake design avoiding squeal. From the outcomes of these calculations design modifications have been derived which have been tested by TRW Automotive. The dependence of squeal occurrence on brake pressure has been predicted by the theoretical model.

1 Mechanisms of Squeal

The phenomenon of brake squeal can be described by means of self-induced vibrations. In the state of squealing there is an energy transfer from the rotational motion of brake parts to the vibrational system of the complete brake. This energy transfer is controlled by the vibrational motion itself.

Table 1 shows three basic excitation mechanisms which can be derived from the brake models to be found in the literature, which has been examined in [1]. In order to find the most suitable mechanism to describe self-induced vibrations of the brake under investigation, those mechanisms have to be examined in detail.

Table 1: *Excitation mechanisms of brake squeal and related criteria for instability*

Friction Characteristic	Geometric Instability	Noncons. Restoring Forces
		
$\left. \frac{d\mu}{dv_{rel}} \right _{\dot{x}=0} < -\frac{d}{F_n}$	$\mu > \tan(\gamma) + \frac{2d_2}{\sin(2\gamma)d_1}$	$\mu > \frac{s}{h} + \frac{c_2}{hsc_3} + \frac{c_2}{hsc_1}$

1.1 Friction Characteristic

Early attempts to explain brake squeal considered the properties of the friction contact to be the reason for the generation of squeal, see for example the work of MILLS [2]. If the force created by sliding friction decreases with increasing relative velocity between the friction interfaces, this might lead to an increasing amplitude in a vibrational system. In [3] this effect is studied in detail using the simple mechanical model of an 1-DOF oscillator sliding on a moving belt.

Depending on the μ, v -characteristic one gets different results, so for the stability behaviour here are two basic characteristics under investigation. First, the Coulomb characteristic, which consists of a distinct static coefficient of friction and a lower constant dynamic coefficient of friction, is regarded. In the sliding case there is no change in the friction force due to sliding velocity and so the equilibrium position is stable. Neglecting structural damping, there is an infinite number of stable attractors with peak velocities smaller than the belt velocity. If the relative velocity becomes zero and the static friction force is higher than the spring force at the moving mass sticking occurs. This state continues until the spring force exceeds the static friction force maximum and the mass starts sliding until it switches back to sticking. This stick-slip limit cycle separates the region of stable vibrations from that part of the state space where the system shows contracting trajectories.

Diverging trajectories can be found in the case of a continuously falling friction characteristic in the vicinity of the equilibrium position, see Fig. 1a). This case contains a stick-slip limit cycle also, and the state space outside this attractor could show diverging trajectories as well as

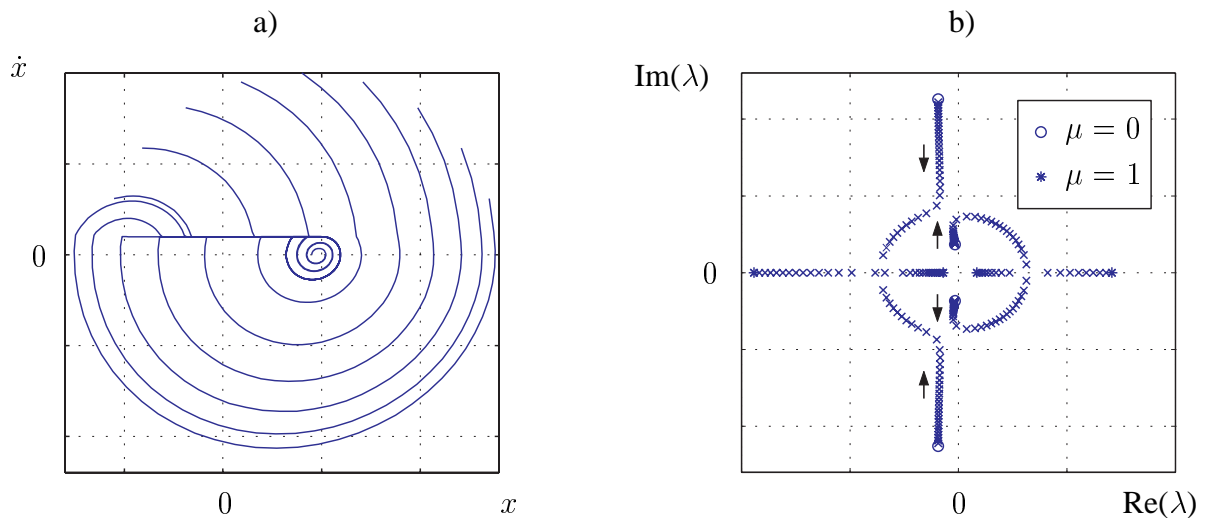


Figure 1: *Stability properties of excitation mechanisms*

- a) *Phaseplane of 1-DOF friction oscillator with linear falling friction-velocity characteristic*
 b) *Root locus plot of 2-DOF System showing the effect of nonconservative restoring forces*

contracting depending on the system parameters.

If a stick-slip limit cycle is assumed to be the reason for squeal, the frequency of the limit cycle should be independent of the belt velocity. This is necessary because experiments show that the frequency of squeal does not change with the rotational speed of the disc. In the case of a Coulomb friction characteristic this feature does not hold and so this explanation of squeal does not appear to be adequate.

Assuming a linear falling characteristic a speed-independent frequency of the limit cycle has been found. For that reason this seems to be a more appropriate mechanism for explaining squeal, although it has to be mentioned that the existence of sticking between disc and brake pad during squeal has not been proven yet.

As it can be seen in Fig. 1a), a continuously falling characteristic leads to an unstable equilibrium position. So for the existence of self excited vibrations the limiting mechanism like changing between sticking and sliding is not important and the falling friction characteristic can be regarded as an excitation mechanism for squeal itself.

1.2 Geometric Instability

Based on experimental investigations in the squeal of brakes of subway-trains, SPURR in [4] developed a hypothesis about the nature of squeal, which is related to the effect of locking

in static systems. An important feature of this mechanism is the angle between the resulting force at the friction contact and the normal direction of the sliding surface. This angle can be defined by geometrical means. SPURR himself did not publish a theoretical model showing the mechanism that he called sprag-slip. Instead, he accepted an suggestion of CRISP, which can be seen in Tab. 1. From this linear model a condition for instability can easily be derived, it is shown below the model. As it can be seen, the stability boundary of the friction coefficient depends strongly on the already mentioned angle and on the damping coefficient. The given expression is only valid for positive angles, in case of an negative angle the relation has to be inverted. Having a closer look at the expression it can be found that for realistic stability boundaries the damping d_1 of the disc should be bigger than the damping d_2 of the pad. This is a property which hardly can be observed in real systems. Therefore, this approach does not seem to be very promising in explaining squeal.

1.3 Nonconservative Restoring Forces

One of the earliest work based on nonconservative restoring forces was done by NORTH [5] in 1972, followed by many other investigations up to recent time, see for example [6]. In Tab. 1 a minimum Model of this mechanism with two degrees of freedom is given. Looking at the equations of motion for this system,

$$\begin{aligned}
 & \underbrace{\begin{bmatrix} m & 0 \\ 0 & J \end{bmatrix}}_{\mathbf{M}} \begin{bmatrix} \ddot{x} \\ \ddot{\varphi} \end{bmatrix} + \underbrace{\begin{bmatrix} d_1 & 0 \\ 0 & d_2 \end{bmatrix}}_{\mathbf{D}} \begin{bmatrix} \dot{x} \\ \dot{\varphi} \end{bmatrix} \\
 & + \underbrace{\begin{bmatrix} c_1 + c_3 & -c_3 s \\ (\mu h - s)c_3 & (s - \mu h)c_3 s + c_2 \end{bmatrix}}_{\mathbf{C}} \begin{bmatrix} x \\ \varphi \end{bmatrix} = 0, \tag{1}
 \end{aligned}$$

it can be realized that friction creates an unsymmetric stiffness matrix indicating nonconservative forces. Because of these forces instability might occur. Using the Hurwitz criterion, five expressions describing stability boundaries for the coefficient of friction can be found. Here, only one is given due to limited space. If the coefficient of friction is varied, and the corresponding eigenvalues are plotted in the complex plain, the effect of mode coupling can be observed, see Fig. 1b). Increasing the coefficient of friction makes the frequencies of the complex modes grow closer until the real parts move in opposite directions and instability occurs.

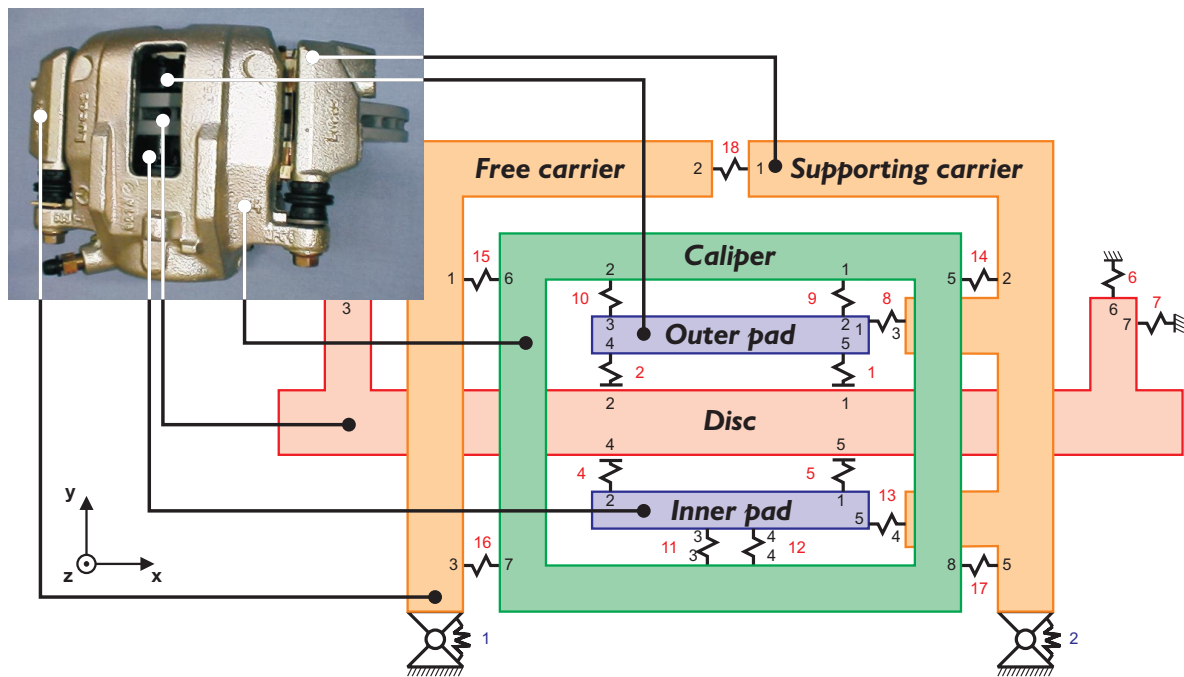


Figure 2: 14 DOF model of a floating caliper disc brake

This mechanism does not need the assumption of sticking in the friction contact and is not dependent on certain damping properties. Looking at the given instability criterion it can be seen that geometry plays an important role defining the stability boundaries. Therefore, the influence of geometric properties on the stability which is known from experiments is included in the mechanism of nonconservative restoring forces. So, this approach seems to be a rather good way describing brake squeal.

2 Brake Model

In order to find design recommendations for brakes avoiding squeal, it is necessary to work with mechanical models displaying design features of a brake. Here, the investigations focus on a floating caliper type disc brake. For this brake a 14 DOF multibody model has been developed. This approach cannot mirror each detail of the brake design but allows an easy variation of design features to check their influence on squeal generation. This is an advantage over the finite element brake models which used in many commercial applications are derived from CAD-drawings and require a lot of effort to do substantial changes in the geometry of components. On the other hand the results from a rather rough model are more general than those from a

detailed FE model for a specific brake design.

So the rigid body system presented in Fig.2 is a link between the very general excitation mechanisms and the specific FE models of a brake.

2.1 Model Structure

As it can be seen in Fig.2, the model consists of 6 rigid bodies which are connected by coupling elements. In general each body has 3 DOF referring to planar motion. As rather high frequencies are regarded, elastic modes of certain components have to be considered. This is done at the carrier by splitting it up into two rigid bodies connected by a coupling element. The stiffness and inertia properties of the disc in the model are chosen in such a way that the representation in the model has eigenfrequencies which are close to frequencies of elastic modes of the disc, known from FEM analysis. The coupling elements connect the bodies by moments or forces, which are dependent on relative displacements and velocities. These dependencies can be linear or nonlinear.

As the displacement amplitudes in a squealing brake are in the order of 10^{-6} m, nonlinear geometric relations can be neglected in calculating displacements, at a first stage.

Frictional contacts are introduced between disc and pads, the assumed coefficient of friction has a constant value. Thus, the frictional forces are proportional to normal contact forces and are oriented into the positive x-direction at the pads, while reaction forces at the disc point into the opposite direction.

2.2 Multibody Algorithm

Since it should be possible to record coupling forces during numerical integration, the Newton-Euler approach is chosen to describe the system's dynamics. By this approach the simulation code gets a transparent structure as the force laws can be formulated for each coupling element explicitly.

For each body i Newton's law gives

$$\mathbf{F}_i = \mathbf{m}_i \ddot{\mathbf{x}}_i, \quad (2)$$

and in case of rotational motion

$$\mathbf{M}_i = \mathbf{J}_i \ddot{\phi}_i. \quad (3)$$

In this expression the reference point is either the center of mass or a point at rest. Vectors

$$\mathbf{x}_i = \begin{bmatrix} x_i \\ y_i \\ z_i \end{bmatrix} \quad \text{and} \quad \phi_i = \begin{bmatrix} \zeta_i \\ \theta_i \\ \varphi_i \end{bmatrix} \quad (4)$$

describe the displacements of the center of mass referring to the inertial frame and angles about the principal axes. These coordinates stand for the degrees of freedom. In the case of the brake model only x_i, y_i and ζ_i are of interest.

So the inertia matrices are

$$\mathbf{m}_i = \begin{bmatrix} m_i & 0 & 0 \\ 0 & m_i & 0 \\ 0 & 0 & m_i \end{bmatrix} \quad \text{and} \quad \mathbf{J}_i = \begin{bmatrix} J_{xx} & 0 & 0 \\ 0 & J_{yy} & 0 \\ 0 & 0 & J_{zz} \end{bmatrix}. \quad (5)$$

The forces

$$\mathbf{F}_i = \sum_j \mathbf{F}_{ij}^k + \mathbf{F}_i^n \quad (6)$$

acting upon a body are composed of coupling forces \mathbf{F}_{ij}^k , which are due to coupling elements connected to contact point j and external forces \mathbf{F}_i^n acting upon the center of mass.

Torques in equation (3)

$$\mathbf{M}_i = \sum_l \mathbf{M}_{il}^k + \sum_j \mathbf{r}_{ij} \times \mathbf{F}_{ij}^k + \mathbf{M}_i^n \quad (7)$$

consist of torques due to couplings to other bodies \mathbf{M}_{il}^k and coupling forces \mathbf{F}_{ij}^k , which are multiplied by coordinates \mathbf{r}_{ij} of the contact points referring to body local frame in the pivot point of the body. Further, there are external torques \mathbf{M}_i^n .

For example bodies $i = 1$ and $i = 2$ are connected at the connecting points $j = 6$ and $j = 4$ by the force coupling element with the index $g(1, 6, 2, 4)$. Similarly, a torque coupling element $h(3, 7)$ links bodies 3 and 7. Thus, the topology of the model is defined by the coupling tables g and h .

Coupling forces \mathbf{F}^e and torques \mathbf{M}^e

$$\mathbf{F}_g^e = \mathbf{f}_f(\mathbf{u}_{i1j1} - \mathbf{u}_{i2j2}, \dot{\mathbf{u}}_{i1j1} - \dot{\mathbf{u}}_{i2j2}) = \mathbf{f}_f(\Delta \mathbf{u}, \Delta \dot{\mathbf{u}}) \quad (8)$$

$$\mathbf{M}_h^e = \mathbf{f}_m(\phi_{i1} - \phi_{i2}, \dot{\phi}_{i1} - \dot{\phi}_{i2}) = \mathbf{f}_m(\Delta \phi, \Delta \dot{\phi}) \quad (9)$$

are calculated using relative displacements and velocities of the linked connecting points. Assuming small displacements, the translational motions of the connecting points

$$\mathbf{u}_{ij} = \mathbf{x}_i + \phi_i \times \mathbf{r}_{ij} \quad (10)$$

$$\dot{\mathbf{u}}_{ij} = \dot{\mathbf{x}}_i + \dot{\phi}_i \times \mathbf{r}_{ij} \quad (11)$$

can be derived from the coordinates \mathbf{x}_i, ϕ_i of the center of mass. Also, the coupling forces and torques can be easily transformed into a representation referring to a body local frame using Newton's third law:

$$\mathbf{F}_{i1j1}^k = -\mathbf{F}_g^e \quad (12)$$

$$\mathbf{F}_{i2j2}^k = \mathbf{F}_g^e \quad (13)$$

$$\mathbf{M}_{i1}^k = -\mathbf{M}_h^e \quad (14)$$

$$\mathbf{M}_{i2}^k = \mathbf{M}_h^e. \quad (15)$$

In case of linear force characteristics the coupling between bodies,

$$\mathbf{F}_g^e = \mathbf{C}_g \Delta \mathbf{u} + \mathbf{D}_g \Delta \dot{\mathbf{u}}, \quad (16)$$

$$\mathbf{M}_h^e = \mathbf{C}_h^m \Delta \phi + \mathbf{D}_h^m \Delta \dot{\phi}, \quad (17)$$

can be described by the symmetric stiffness matrices $\mathbf{C}_g, \mathbf{C}_h^m$ and damping matrices $\mathbf{D}_g, \mathbf{D}_h^m$.

Incorporation of a friction force between bodies, which is orthogonal to the axis of the coupling element, leads to an asymmetric matrix \mathbf{C}_g .

2.3 Simulation Software

The simulation software should meet the following requirements:

- fast numerical integration
- flexibility concerning the structure of the mechanical model
- possibility of linear eigenvalue analysis
- easy incorporation of nonlinear relations
- visualization of calculation results
- open to future improvement

Therefore, ACSL (Advanced Continuous Simulation Language) was chosen as a base for simulation. This language was developed for description and simulation of ODEs, it uses efficient

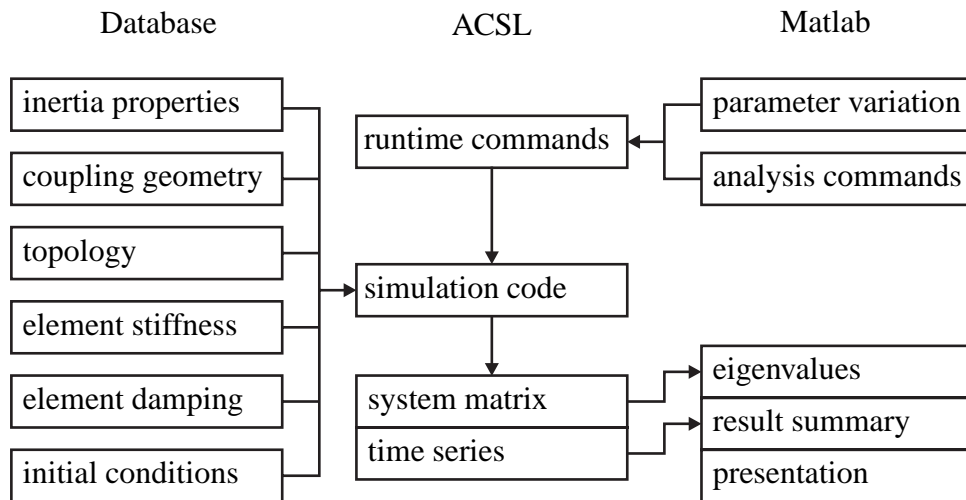


Figure 3: *Structure of simulation software*

Fortran compilers for generating machine code. ACSL offers different integration algorithms and includes an automatic time step control to incorporate discrete events into the integration procedure.

Since it should be possible to change the structure of the model easily, the defining parameters are stored in separate files. So the model data is accessible to other programs, for example to Maple for doing symbolic calculations. This was used to check the simulation algorithm programmed in ACSL.

The simulation code is framed by Matlab programs which on one hand contain analyzing commands for ACSL and on the other hand evaluate and visualize the results of the calculations. An overview over the simulation software can be seen in Fig. 3.

2.3.1 Simulation Code

Using the algorithm described in 2.2, the governing structure of the program is a loop stepping through all coupling elements computing the coupling forces. These forces are summed up and give the body accelerations, which are integrated. As the brake model is a planar description of the real system, there are only three DOFs x_i, y_i, φ_i for each body. These coordinates and their time derivatives stand for the system states. To achieve a consistent description of the mechanical system, the inertial frame is connected to a rigid body at rest.

Table 2: *Determination of Model Properties*

Model Properties	Sources
topology	brake's geometry, modal vibration patterns
inertia properties brake disc, carrier caliper, pad	measured eigenfrequencies, stiffness values calculated from FEM measured masses, moments of inertia
position of connecting points	experimental determination of the center of mass, geometry of components, torsional stiffness values of FE-model
stiffness values	FE-model
damping values	experimental modal analysis
coefficient of friction	measured values

2.3.2 Test of Simulation Code

In order to check the correctness of the ACSL code, linear test models have been defined. These models have been described by the ACSL simulation software on one hand and on the other hand their equations of motion have been derived by Lagrange's equations of second kind. The second way was performed using the algebraic manipulation program Maple. Using the same parameters, the eigenvalues of the system matrix were calculated for each description separately. The comparison of results showed negligible differences only.

2.3.3 Determination of Parameters

Parameter values have been determined by measurements conducted at brake components or by calculations using a validated FE-model of the brake under investigation. By applying static forces to brake components and calculating the resulting deflections the stiffness of the coupling elements has been found. Table 2 shows the methods used to determine the different parameters.

3 Brake Noise Test Rig

For investigation of a real brake system and for verifying simulation results a brake noise test rig has been built, see Fig. 4. This experimental setup is able to conduct noise tests automatically

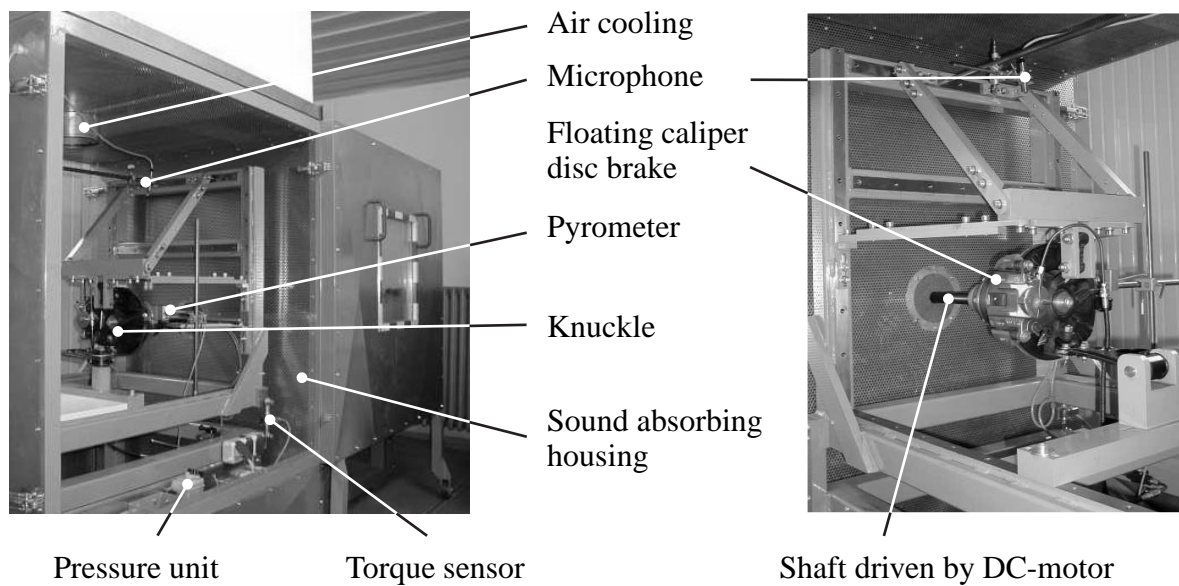


Figure 4: *Brake noise test rig*

and can be adapted to other objects of investigation.

3.1 Mechanical Setup

To avoid mistuning of the brake dynamics, the knuckle of a front wheel of a Mercedes-Benz A-class car has been incorporated into the setup. Brake and knuckle are connected to a L-shaped frame which is fixed to the substructure at four corners by three brackets and a force sensor. So, small elastic deflections are used to determine the brake torque. Due to the brackets the L-shaped frame can be exchanged for other setups easily.

The wheel shaft carrying the brake disc is directly driven by a 84kW DC-Motor using a continuous speed universal-joint propeller shaft. This setup avoids any sound and vibration coming from the gear box. The power supply of the motor is done via a digital controller which is able to generate speed ramps.

As described in [7], brake pressure is generated using a main cylinder from a car. This cylinder is driven by an electronically controlled pneumatic actuator and can generate up to 40bar of line pressure.

The brake setup as well as the pressure unit are surrounded by a sound absorbing housing with sliding doors. If the doors are closed, the air taken from the cabin by the air cooling ventilator creates a depression. This depression forces air from the environment of the housing to enter

The screenshot shows a software window titled "VS:Bremsreihe" with the following configuration:

- Name: Matrix
- Abarbeitung: Schleifenweise
- Schleifenfolge: Temp.->Drehzahlen->Drücke
- Temperaturkonditionierung

Temperaturen		Drehzahlverläufe			Bremsdruck-Arbeitspunkte	
T [°C]	t [s]	n1 [1/min]	n2 [1/min]	p [bar]		
0 50	0 10	40	40	0 5		
1 100	1			1 10		
2 150	2			2 15		
3 200	3			3 20		
4 250	4			4 25		

Additional parameters:

- Maximaltemperatur: 500
- Abkühltemperatur: 480
- Sampling-Rate [Hz]: 40000
- Bremsdruck-Zeitfunktion: Rampe
- Bremsdruck-Amplitude [bar]: 5

Measurement channels:

- A/D CH 0 Meßwerterfassung
- A/D CH 1 Meßwerterfassung
- A/D CH 2 Meßwerterfassung
- A/D CH 3 Meßwerterfassung

Decimals (Dezimierung):

- A/D CH 0 Dezimierung: 40
- A/D CH 1 Dezimierung: 40
- A/D CH 2 Dezimierung: 40
- A/D CH 3 Dezimierung: 40

Figure 5: Dialog for programming of test sequences

the cabin by a flexible aluminium pipe which directs the airflow towards the brake for cooling. In this way a maximum air flow of $1000\text{m}^3/\text{h}$ can be reached.

Within the cabin there is a b&k microphone including a preamplifier to pick up the time signal of occurring noise. To measure the temperature of the brake disk, a pyrometer is used. Compared to the alternative approach of a sliding thermo couple the noncontact thermometer avoids the sliding noise, does not influence the vibrational properties of the disc and gives a rather fast response to thermal changes.

3.2 Control and Data Processing

Data acquisition and control of the test rig is done using a PC including special I/O-hardware supported by a realtime computer. Acquisition and control software on the PC has been developed using the TestPoint environment which allows object oriented programming. This software is described in [8] and has to deal with several tasks:

- recording of measurement data
- digital filtering of measurement data
- visualizing of recorded data

- managing of recorded data
- programming of drive controller via serial port
- control of test parameters like rotational speed and brake pressure
- online display of sampled data

Most of the given tasks can be operated in manual or in automatic mode. In manual mode an operator interacts directly with the software to conduct single measurements. To investigate brake squeal it is necessary to do test sequences consisting of many brakings to find out about the statistics of noise generation. Therefore an automatic mode was implemented, which means that the testrig runs under program control. Test sequences can be programmed using the dialog shown in Fig. 5. Defining a testing sequence, the measurement signals which have to be recorded are set. Lists are used to constitute the values for rotational speed, brake pressure and disc temperature giving different operation conditions of the brake. It is possible to switch between different loop hierarchies concerning the course of parameter variation. Single testing sequences can be arranged to a testing program. Recorded data is stored in binary files which are further evaluated using Matlab on HP workstations.

For security reasons the automatic mode is monitored by a realtime computer programmed in Pearl. By checking the measurement signals for consistency it is decided whether the testing procedure has to be cancelled or not, referring details can be found in [9].

4 Investigations Based on Nonconservative Restoring Forces

As it has been shown in section 1 that the assumption of nonconservative restoring forces seems to be a rather promising approach explaining brake squeal. Therefore in this project most investigations are based on this assumption.

4.1 Experimental Determination of the Coefficient of Friction

Looking at the terms given in Tab. 1 it has been found that the coefficient of friction (COF) plays an important role in generating brake squeal. In the case of nonconservative restoring forces the absolute value of this parameter is of interest. So the test rig has been equipped with a force transducer which has been calibrated by a lever beam and weights to give the brake torque.

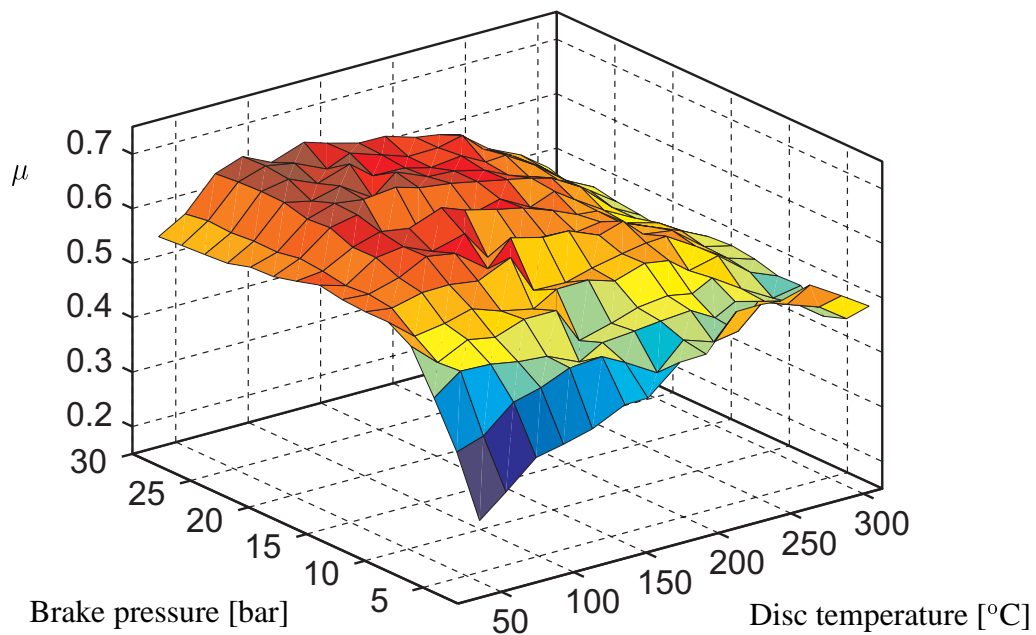


Figure 6: *Coefficient of friction between pad and disc*

Knowing torque and brake pressure, the COF between pad and disc can be calculated using the geometry of the brake system.

To find out the dependence of the COF on brake pressure and disc temperature a test sequence has been conducted which varied pressure from 2 bar to 30 bar and the initial disc temperature covered a range from 50°C to 300°C. Brakings were performed at a constant speed of 40 rpm and had a duration of 10 sec. Before each test sequence a bedding procedure was conducted to adjust the pad surface to the disc and produce realistic contact conditions.

To find the COF for each braking, the sampled data have been averaged. For the same brake configuration the reproducibility of results was quite good. They are shown in Fig.6. It can clearly be seen that in normal operation conditions the value of the COF spreads over a wide range from 0.3 to 0.6. For low pressure, the COF increases with increasing disc temperature, whereas for high pressure a total maximum has been found between 100°C and 150°C. Following the experience of car brake suppliers this is a typical temperature range for brake squeal. On the other hand it can be said that the COF under realistic circumstances might change its value by 100%.

Since the behaviour to the COF is usually dependent on the duty history of the brake system, the sequence of testing has been changed to find out about the reproducibility of results.

In the first testing sequence the disc temperature was kept constant while all of the pressure

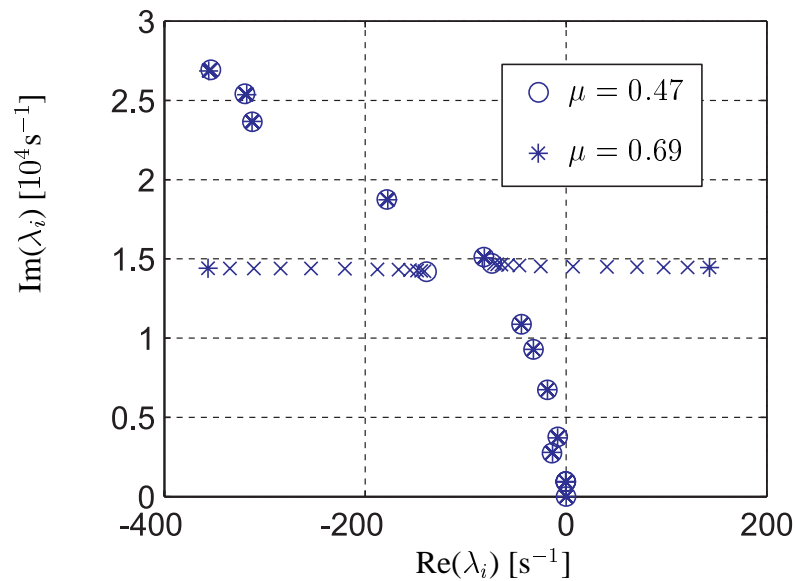


Figure 7: *Instability of brake model due to nonconservative restoring forces*

values belonging to the test were stepped through. To check this result, during the second test sequence successive brakings had the same pressure values but changing disc temperatures. Differences between the results of these two sequences were negligible small.

4.2 Proof of Existence of a stability Boundary

Before analyzing the brake model described in section 2 it has to be checked if the geometry of the brake system allows the existing nonconservative forces to destabilize the mechanical system. This takes into account that the geometry and the inertia properties of the brake components can be determined more exactly than stiffness and damping values of contacts between parts.

For the investigation described in this paragraph geometry and inertia parameters of the brake have been determined as shown in Tab.2 and stiffness and damping properties were set to approximate values in a realistic range. Furthermore, an uneven pad wear was assumed which gave an uneven distribution of stiffness in the pad material of the brake model.

Using this basic model, the coefficient of friction was varied stepwise from 0.47 to 0.69 and for each step the system matrix and its eigenvalues have been calculated. The results are plotted in the complex plane and shown in Fig.7. With the approximate values for stiffness and damping the destabilisation of the brake model occurs at a COF of $\mu = 0.64$, which is a realistic value.

Calculating the frequency of the unstable mode, one finds a value of $f = 2400\text{ Hz}$, which also is a realistic squeal frequency. Besides this lifelike values the effect of mode coupling can clearly be seen.

Thus by this study it has been proven that nonconservative forces can lead to unstable vibrations in the given brake design.

4.3 Sensitivity Analysis

Introducing the more exact stiffness values derived from the FE-Model, the brake model becomes more accurate, but parameter values for damping elements are still difficult to determine. Therefore, damping values have been assumed, so that the over all damping value of the brake system corresponds to the average of measured values achieved from experimental modal analysis. With this assumed damping values it is not possible to calculate reasonable stability boundaries, but the mechanism of nonconservative restoring forces is a matter of stiffness and geometry properties which are known better. Thus, it appears to be more reasonable to find out how much the stability of the system is affected by a variation of a certain parameter than to calculate the parameter value at which the system becomes unstable. Therefore a sensitivity analysis is conducted.

4.3.1 Basic Considerations

Regarding the stability of the brake model, the sensitivity of eigenvalues to parameter variations has to be considered.

Using a state space model for the mechanical system under investigation results in

$$\dot{\mathbf{x}} = \mathbf{A}\mathbf{x}. \quad (18)$$

If \mathbf{v}_i is the eigenvector assigned to eigenvalue λ_i , it follows that

$$\mathbf{A}\mathbf{v}_i = \lambda_i\mathbf{v}_i. \quad (19)$$

Similarly one finds for the eigenvector \mathbf{w}_k of the transposed system matrix \mathbf{A}^T

$$\mathbf{w}_k^T \mathbf{A} = \lambda_k \mathbf{w}_k^T. \quad (20)$$

There is a relationship between the eigenvectors \mathbf{v}_i and the adjoint eigenvectors \mathbf{w}_i , which is

$$\mathbf{v}_i^T \mathbf{w}_j = \mathbf{w}_j^T \mathbf{v}_i = \delta_{ij}, \quad (21)$$

where δ_{ij} stands for Kronecker's delta. Partial differentiation of (19) with respect to a parameter p gives

$$\frac{\partial \mathbf{A}}{\partial p} \mathbf{v}_i + \mathbf{A} \frac{\partial \mathbf{v}_i}{\partial p} = \frac{\partial \lambda_i}{\partial p} \mathbf{v}_i + \lambda_i \frac{\partial \mathbf{v}_i}{\partial p}. \quad (22)$$

Multiplying this equation by the transposed adjoint eigenvector leads to

$$\mathbf{w}_i^T \frac{\partial \mathbf{A}}{\partial p} \mathbf{v}_i + \mathbf{w}_i^T \mathbf{A} \frac{\partial \mathbf{v}_i}{\partial p} = \mathbf{w}_i^T \frac{\partial \lambda_i}{\partial p} \mathbf{v}_i + \mathbf{w}_i^T \lambda_i \frac{\partial \mathbf{v}_i}{\partial p}. \quad (23)$$

Using equation (20) and $i = k$ the sensitivity of an eigenvalue λ_i with respect to a parameter p can be expressed by

$$S_p(i) = \frac{\partial \lambda_i}{\partial p} = \frac{\mathbf{w}_i^T (\partial \mathbf{A} / \partial p) \mathbf{v}_i}{\mathbf{w}_i^T \mathbf{v}_i}, \quad i = 1, 2, \dots, n. \quad (24)$$

Thus an analytical description of the eigenvalue sensitivity based on the system matrix sensitivity becomes possible, additional information can be found in [10].

Equation (24) needs eigenvectors or eigenvalues to determine sensitivity. For a parameter change Δp of technical relevance the system eigenvalues and eigenvectors are changing by a significant amount. So the sensitivity can not be calculated by equation (24).

On the other hand, modern computer systems allow an easy way of calculating eigenvalues of even large matrices. So it is an workable approach to determine system eigenvalues before and after a variation Δp and calculate the difference $\Delta \lambda$ directly by numerical means. Hence, for this approach the term *technical sensitivity analysis* is introduced.

4.3.2 Parameter Groups

The model under investigation comprises 6 relevant bodies and 18 coupling elements. Therefore it would be an extensive task to vary all the parameters involved separately. Also, it is important to do variations which have a practical meaning concerning design. For both reasons the parameters have been divided into subsets of values which are changed simultaneously by the same amount. These subsets are called parameter groups and are given names of practical meaning. For parameters like stiffness and damping related to coupling elements there are different ways of changing values combined to a group:

- Symmetric variation: values are changed by the same amount and in the same direction.
- Asymmetric variation: values are changed by the same amount but in opposite directions. The asymmetric change can be done clockwise or counter clockwise.

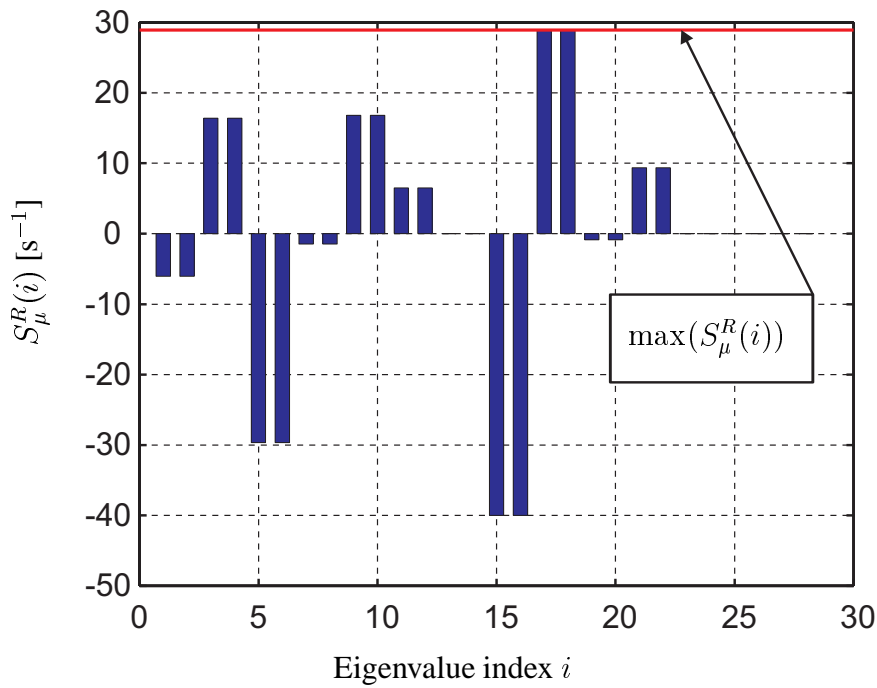


Figure 8: Sensitivity of basic brake design referring to COF variation

4.3.3 Investigation of Robustness

The coefficient of friction (COF) is a parameter of the brake system which can change a lot during operation, see Fig.6. On the other hand it is well known fact under car brake suppliers that a high COF increases the probability of squeal.

Therefore the stability of the brake model is investigated with respect to a change of the COF. Also, it has been found out how certain modifications of the brake design influence the reaction of the model to a COF-variation. In other words the robustness of differently modified brake designs against an increasing COF has been examined.

Robustness of a brake design can be calculated by

$$S_{\mu}^R(i) = \frac{\Delta \operatorname{Re}(\lambda_i)}{\Delta \mu} = \frac{\operatorname{Re}(\lambda_i(\mu_2)) - \operatorname{Re}(\lambda_i(\mu_1))}{\mu_2 - \mu_1} \quad (25)$$

for each eigenvalue λ_i , $i = 1 \dots n$. Doing this, values $\mu_1 = 0.4$ and $\mu_2 = 0.6$ were used. Having a system of $n = 28$ system states, there are 28 sensitivity values calculated according to equation (25). These are equal in pairs as the vibrational system is described by 14 conjugated complex pole pairs.

Studying robustness, design modifications were made by a 10% change of the grouped Parameters. After the sensitivity to the COF was calculated using equation (25), the maximum sensi-

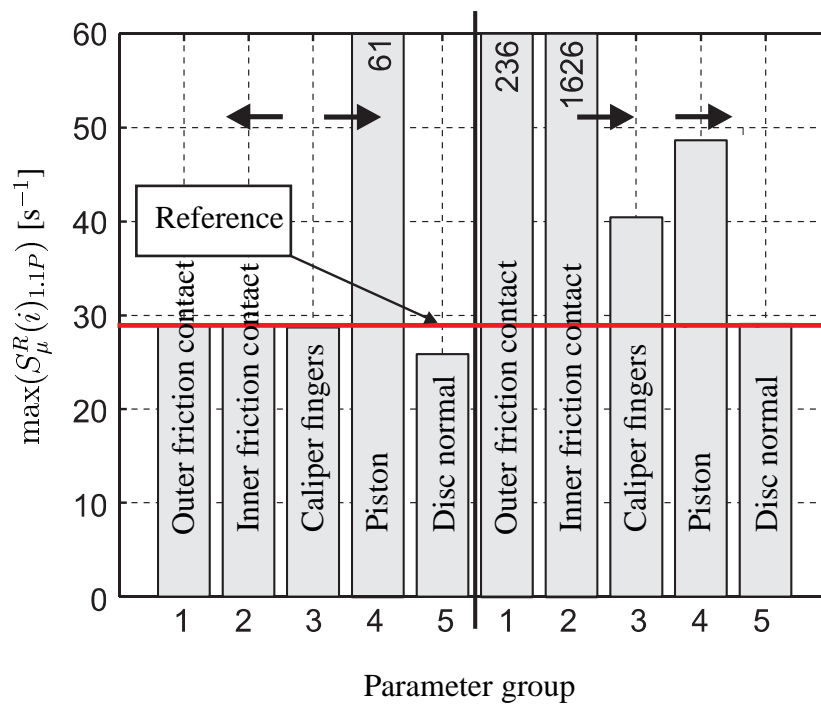


Figure 9: Results of sensitivity analysis concerning robustness for symmetric (→→) and asymmetric (←→) variation of the position of coupling elements

tivity values over all eigenvalues are displayed in a bar diagram. The values given by equation (25) were calculated for the basic brake design also, see Fig. 8, and their maximum is marked in the diagram as a reference. To give an example, the results of the maximum sensitivity values for 10 out of more than 100 design modifications are shown in Fig. 9. This results from a change of the x-coordinates of the connecting points. As only the maximum value of all eigenvalue sensitivities is displayed, a value exceeding the reference does not directly mean that the robustness becomes worse by this modification. Deviations from the reference value only indicate that modifications of the particular parameter group will have a strong influence on system stability.

Looking at the chosen results, it can be seen that properties of the friction contact and the contact between backplate and piston or caliper fingers are important concerning robustness. Especially asymmetric modifications show a strong influence.

The main results from the robustness investigation are:

- Pad properties are important.
- Connections to backplate are important.
- Increase of damping does not always improve robustness.

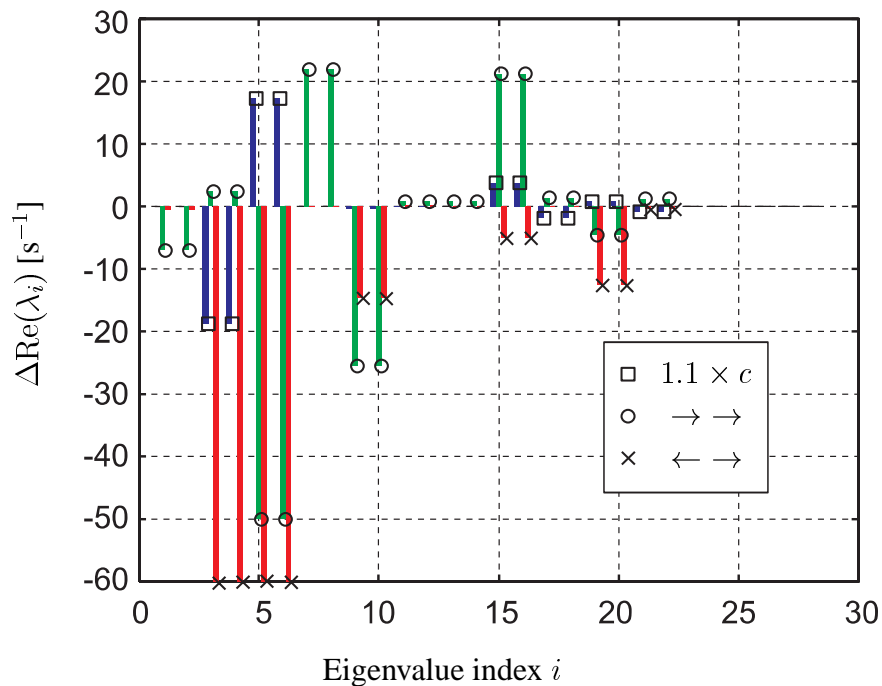


Figure 10: Change of eigenvalue real parts due to variations of parameter group 'piston'

- Positions of connecting points between pad and carrier are important.
- Asymmetric design modifications are mostly prone to squeal than symmetric ones.

As the first three findings are in line with practical experience it can be said that the brake model is able to mirror real features of the brake under investigation.

4.3.4 Investigation of Parameter Influences

Besides the robustness against a varying COF, it is interesting to know how parameter modifications itself affect stability. Therefore parameters were varied in groups as described in 4.3.2 by 10% and the COF between pad and disc was kept at a constant value of $\mu = 0.4$.

The resulting changes of the real parts $\Delta\text{Re}(\lambda_i)$ of eigenvalues due to parameter variation were plotted as a bar diagram over eigenvalue index $i = 1 \dots 28$. Real part changes were not divided by the related parameter difference, because the varying size of parameter values – differences between stiffness and geometry parameters are in an order of 10^9 – would lead to incomparable results.

Figure 10 presents results from modifications of the parameter group 'piston'. These modifications consisted first in a symmetric increase of coupling stiffness values, secondly in an

asymmetric and thirdly in a symmetric displacement of connecting points. As it can be seen, parameter changes can have different effects on the eigenvalue pattern:

- **Narrow band effect:** The first symmetric change affects eigenvalues related to high eigenfrequencies only.
- **Mode Coupling:** Again the symmetric change of stiffness properties shows that adjacent eigenvalues move in opposite directions.
- **Broad band effect:** The asymmetric displacement of coupling elements affects several real parts over a wide frequency range.
- **Monodirectional effect:** The change of stiffness as well as the asymmetric displacement of coupling elements make real parts move in two opposite directions, whereas the real part displacement due to a symmetric shift of coupling elements is in one direction only.

The symmetric shift of coupling elements increasing the distance between those leads to a general stabilisation of the system with a very strong influence in the upper frequency range of the model. This stabilizing effect has been observed in other parameter groups as well and so real brakes have been modified in two ways so that in the first case the distance between two connecting points has been increased and in the second case this distance has been decreased. Both modifications have been compared with respect to their squeal behaviour. In these two tests the first design proved to be less noisy than the second one in the frequency range up to 5 kHz, see the contribution of TRW in this issue: 'Bremsenquietschen' by T. Treyde [11]. Bearing in mind that the model is of a rather simple structure and therefore mainly valid for the lower frequencies of squeal, these results are a good confirmation for the approach chosen in this work.

The main results from the investigations of the parameter influence can be summarized as follows:

- Parameters close to the friction contact play an important role.
- Symmetric increase in damping always stabilizes the system.
- Increase of inertia parameters lowers the stability.
- Increase of distance between two connecting points has a stabilizing effect.

4.4 Influence of Nonlinear Pad Stiffness

Applying the sensitivity analysis as described above it became obvious that parameters in the vicinity of the friction contact have a strong influence on system stability. Therefore it appears to be reasonable to do some refinements in this part of the model.

Measurements conducted during the BMBF-project 'Brake Judder', which is described in this volume under 'Brake Judder of Cars' by C. Schmalfuß et al. [12], showed a nonlinear relationship between compression and normal force at the brake lining. Thus, cubic hardening springs have been incorporated into the simulation algorithm. The corresponding coupling elements were used to connect pad and disc.

The compression amplitudes utilized in the fore mentioned tests were by far larger than the ones occurring during squeal. Therefore it has to be checked if the observed nonlinearity is relevant in the regarded amplitude range.

4.4.1 Computation Procedure

Due to the incorporated nonlinear relationships the linear eigenvalue analysis cannot be applied any more. For this reason the stability behaviour is examined based on numerical integration procedures. Starting with particular initial states the decay or increase of vibration amplitudes is investigated numerically. Since the system comprises 14 coupled degrees of freedom, it is not reasonable to look at time series describing the time history of a single system state. Therefore, a measure for the energy stored in the system is introduced. This measure is called *linear energy* E^l and is defined by

$$E^l(t) = \frac{1}{2} \mathbf{x}^T(t) \begin{bmatrix} \mathbf{K} & \mathbf{0} \\ \mathbf{0} & \mathbf{M} \end{bmatrix} \mathbf{x}(t), \quad (26)$$

where \mathbf{K} and \mathbf{M} are the stiffness and mass matrix of the linearised system, respectively. The stiffness matrix \mathbf{K} is not known a priori, it has to be extracted from the system matrix

$$A = \begin{bmatrix} \mathbf{0} & \mathbf{E} \\ -\mathbf{M}^{-1}\mathbf{K} & -\mathbf{M}^{-1}\mathbf{D} \end{bmatrix} \quad (27)$$

which can be calculated by ACSL.

The initial conditions of the numerical integration have to be chosen in such a way that there is an influence of the included cubic nonlinearity on the system's time history started by these

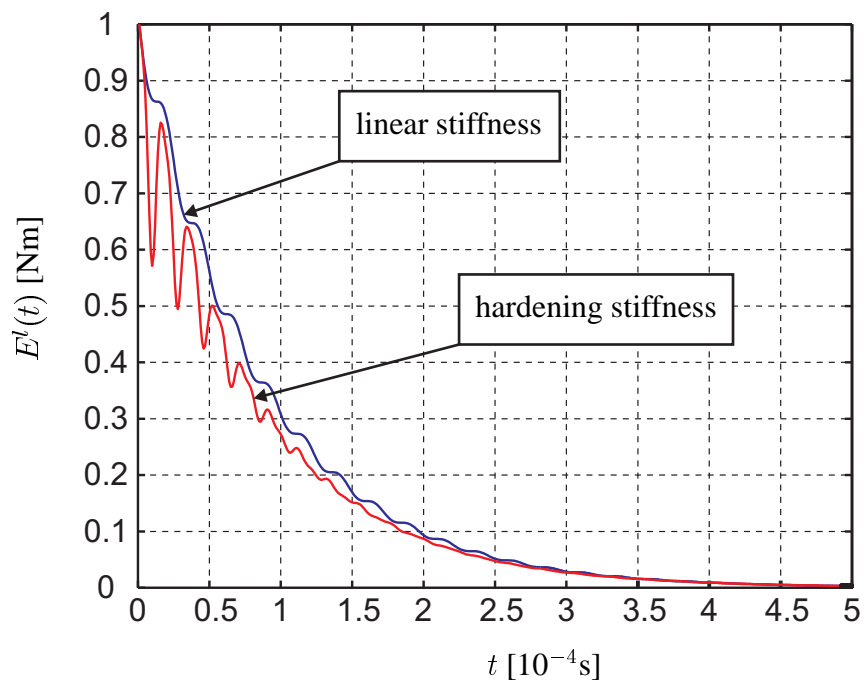


Figure 11: Decay of vibrations in the linear and in the nonlinear case

initial conditions. On the other hand, the numerical investigations should show the systems behaviour as a whole, not only particular motions. For this reason and to keep a certain amount of consistency to the investigation of the linear system modeshapes scaled to $E^l(t = 0) = 1\text{Nm}$ were used as initial conditions. Time series $E^l(t)$ have been calculated for the linear and for the nonlinear case and the results have been compared.

4.4.2 Numerical Results

As it can be seen in Fig. 11 there is an influence of a hardening spring on the rate of energy dissipation. It depends on the initial conditions whether it stabilizes – as it can be realized here – or destabilizes the system. Starting with conditions derived from the eigenvector belonging to the complex eigenvalue pairs $i = 5, 6$, gives the curve shown in Fig. 11. Also stabilizing effects can be observed in the case of $i = 5, 6$. The opposite tendency can be found if vibrations are excited using modeshapes related to eigenvalues $i = 1, 2$ and $i = 3, 4$. Even in the linear case all of the mentioned eigenvectors are sensitive to changes in coupling stiffness connecting pad and disc.

To achieve significant differences between the linear and the nonlinear case in the calculated time series, the factor scaling the cubic term in the nonlinear relation had to be set to unrealistic

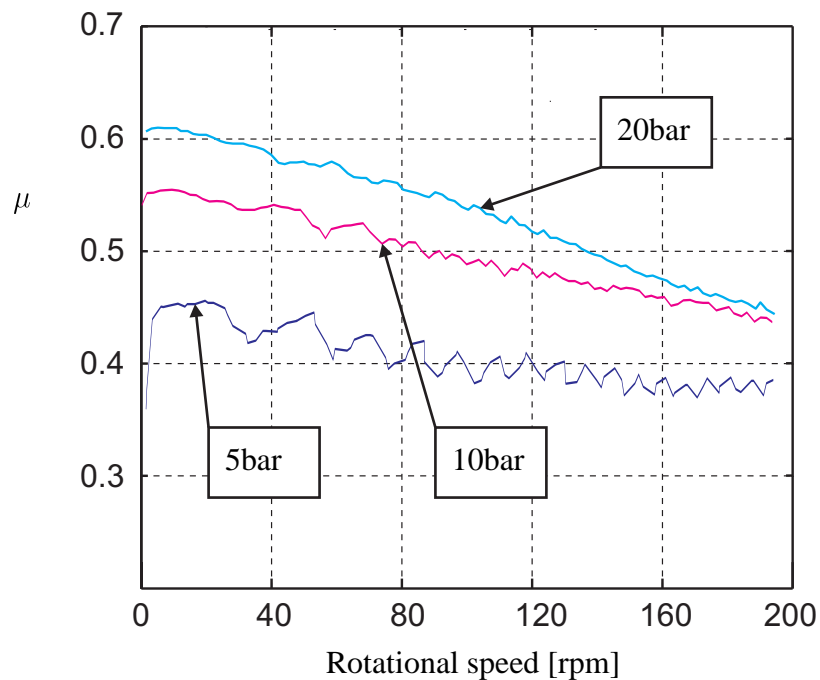


Figure 12: Measured friction characteristics

high values. Therefore, it can be concluded that the nonlinearity under investigation is not very important for the system stability.

5 Investigations Based on a Falling Friction Characteristic

As shown in the preceding section, the mechanism of nonconservative restoring forces leads to results, which are in good agreement with practical experience. On the other hand it was not possible to destabilize the described brake model by a parameter variation in a realistic range. So, a further refinement of the model is needed.

As stated earlier, the vicinity of the friction contact is a very sensitive area and thus it seems to be reasonable to model friction properties more exactly.

5.1 Experimental Results

To find out more about the friction between pad and disc, coefficient of friction was recorded during stop brakings from 200 rpm to 0 rpm in 12 sec. The results are shown in Fig. 12 and it can clearly be seen that there is a nearly linear relationship between the coefficient of friction and the rotational speed of the disc. This relationship depends on brake pressure and on disc tem-

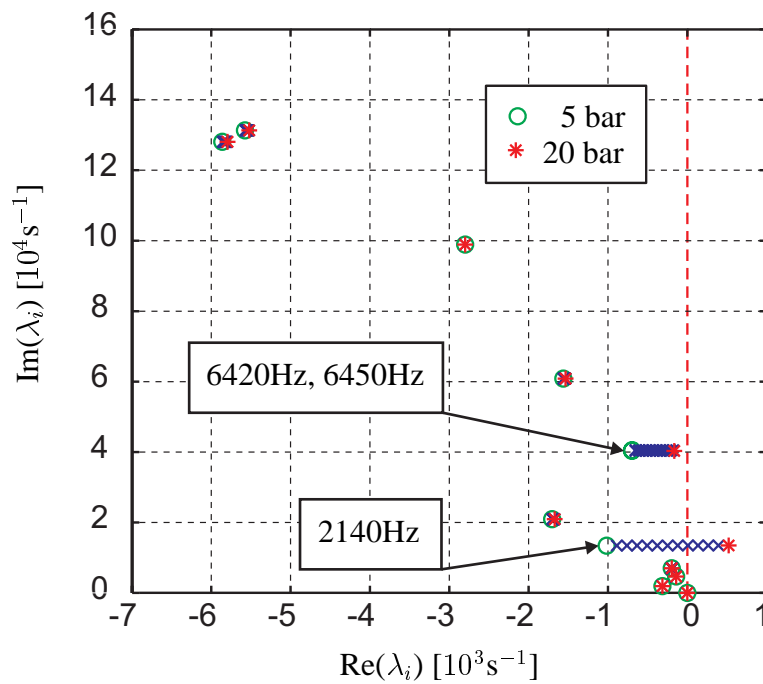


Figure 13: *Destabilisation due to falling friction characteristic*

perature, but the falling characteristic can be realized in nearly any case, even if an accelerated motion is regarded and temperature effects are compensated. For further details see [13].

5.2 Model Calculations

A falling friction characteristic is a mechanism to generate squeal. It can be studied in detail using a 1-DOF oscillator sliding on a moving belt, displayed in Tab.1. A velocity dependent coefficient of friction can be given by

$$\mu(v_{rel}) = \mu_0 - k|v_{rel}|, \quad (28)$$

where the relative velocity $v_{rel} = v_0 - \dot{x}$ is the difference between belt-velocity v_0 and the velocity of the mass \dot{x} . Here, μ_0 stands for the coefficient of static friction and k for the slope of the friction characteristic.

Ignoring viscous damping, the equation of motion for the sliding friction oscillator reads

$$m\ddot{x} + cx = \mu(v_{rel})F_n \text{sgn}(v_{rel}), \quad (29)$$

with the normal force F_n . Equation (29) can be transformed using dimensionless time $\tau = \sqrt{c/mt}$ to

$$x'' + 2Dx' + x = \frac{F_n}{c}(\text{sgn}(v_{rel})\mu_0 - kv_0), \quad (30)$$

where $(\dots)' = \frac{d}{d\tau}(\dots)$ and

$$D = -\frac{F_n k}{2\sqrt{cm}} < 0. \quad (31)$$

It becomes obvious, that due to the friction characteristic negative damping occurs. This damping is dependent on the dynamic parameters m, c , as well as on the slope k and on the normal force F_n .

Applying this to the brake model yields a negative damping which varies with brake pressure. For the slope an average value of $k = 0.0576 \text{ sm}^{-1}$ has been taken from the measurements. A stability analysis with changing brake pressure from 0 bar to 25 bar was conducted and it was found that instability occurs at a brake pressure of about 15 bar and a mode frequency of 2140 Hz. Figure 13 shows the calculation results in a section of the complex plain.

5.3 Experimental Verification

To get an impression of the squeal behaviour of the brake under investigation, a test sequence of 225 brakings has been programmed and performed. This sequence comprised a pressure range from 2 bar to 30 bar and a temperature range from 30°C to 310°C, while brakings were performed at a constant speed of 40 rpm and lasted for 12 sec. For each braking the noise was recorded and analyzed by FFT. Sounds of a sound pressure level higher than 60 dB were extracted as a noise event. Those events have been plotted versus frequency and brake pressure in Fig. 14. It can be realized that a squeal noise of 2350 Hz has been found at pressures starting at about 12 bar, which is remarkably close to the predicted squeal range starting at 15 bar with a noise frequency of 2140 Hz.

In summary it can be concluded that using a falling friction characteristic even a rather simple brake model can display important details of squeal noise occurrence.

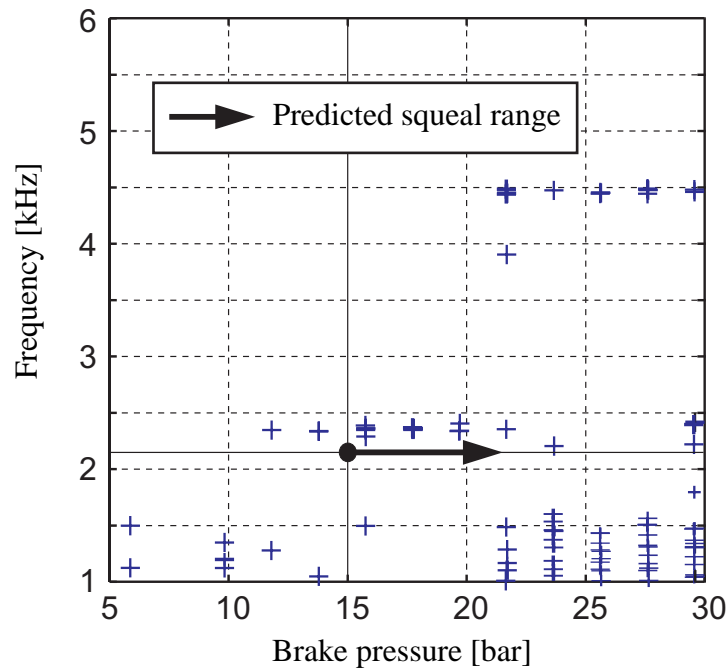


Figure 14: Squeal occurrence ($spl > 60$ dB) depending on brake pressure

6 Summary

The work described in this report can be divided into two main parts. First the development and installation of tools to deal with the phenomenon of brake squeal. Secondly the analysis of this phenomenon by theoretical and experimental means using the tools developed.

The main theoretical tool to deal with brake squeal is a simulation software based on a general multibody algorithm. This software has been used to describe a 14-DOF model of a floating caliper brake. As an experimental tool an automatically controlled brake noise test rig has been installed and operated. Two different excitation mechanisms of squeal generation derived from literature have been incorporated into the brake model.

First, nonconservative restoring forces gave the base for a sensitivity analysis showing the influence of parameter variations on the system stability. The results of this investigation were in good agreement with practical experience and lead to design recommendations how to achieve a more silent brake. Especially increasing the distance between connecting points of components in the plane, which is parallel to the rubbing surface of the disc, can improve the dynamic stability of a brake.

The second excitation mechanism included in the brake model is a falling friction characteris-

tic, where the parameters have been determined by experiments using the brake noise test rig. It has been shown that by this mechanism the dependence of squeal on brake pressures can be predicted quite exactly.

So, as a conclusion two main results can be stated:

- Using the excitation mechanism of nonconservative restoring forces, effective design recommendations for a silent brake can be derived even from a simple brake model.
- The occurrence of squeal depending on brake pressure can be predicted based on the excitation mechanism of a falling friction characteristic.

During the work described above it became very clear that the complex problem of brake squeal needs an intense combination of experimental and theoretical investigations. There is still a lot of work to be done to design a completely silent brake, but this survey bore tools, methods and knowledge which are a fertile base for this aim.

7 Acknowledgements

This study is funded by the 'Bundesministerium für Bildung und Forschung'. The authors are grateful for this support. Furthermore the authors would like to thank Dr. T. Treyde, J. Korte and A. Stache of TRW for their fruitful discussions.

References

- [1] RUDOLPH, M. and K. POPP: *1. Zwischenbericht zum BMBF-Verbundprojekt, Teilprojekt III: Beeinflussung und Vermeidung reibunsselbsterregter Schwingungen*. Technical Report, Universität Hannover, Inst. f. Mechanik, 1998. FKZ: 13N7202.
- [2] MILLS, H. R.: *Brake squeak*. Technical Report 9000 B, 9162 B, Inst. of Automobile Engineers, 1938,1939.
- [3] RUDOLPH, M. and K. POPP: *2. Zwischenbericht zum BMBF-Verbundprojekt, Teilprojekt III: Beeinflussung und Vermeidung reibunsselbsterregter Schwingungen*. Technical Report, Universität Hannover, Inst. f. Mechanik, 1998. FKZ: 13N7202.
- [4] SPURR, R. T.: *A Theory of Brake Squeal*. Proc. Instn. Mech. Engrs., 1:33–40, 1961.
- [5] NORTH, M. R.: *Disc Brake Squeal - A Theoretical Model*. Technical Report, MIRA, 1972. No. 1972/5.
- [6] ALLGAIER, R., L. GAUL, W.KEIPER and K. WILLNER: *Mode lock-in and friction modelling*. In GAUL, L. and C. A. BREBBIA (editors): *Computational Methods in Contact Mechanics IV*, pages 35–47, Southampton, Boston, 1999. WIT Press.
- [7] GIERSE, A.: *Entwurf und Bau einer Bremsdruck-Steuerung*. Studienarbeit am Institut für Mechanik, Universität Hannover, 1999.
- [8] FARNUNG, M.: *Entwicklung und Realisierung einer Versuchsstand-Steuerung mit Messgrößenerfassung*. Diplomarbeit am Institut für Mechanik, Universität Hannover, 1999.
- [9] CLAUSEN, M.: *Entwurf und Umsetzung einer Funktionsüberwachung für einen Bremsenprüfstand*. Studienarbeit am Institut für Mechanik, Universität Hannover, 1999.
- [10] FRANK, P. M.: *Introduction to System Sensitivity Theory*. Academic Press, New York, San Francisco, London, 1978.
- [11] TREYDE, T.: *Bremsenquietschen*. In POPP, K. (editor): *Detection, Utilization and Avoidance of Nonlinear Dynamical Effects in Engineering Applications*, pages 227–244. Shaker Verlag, Aachen, 2001.
- [12] SCHMALFUSS, C., A. AMS and W. WEDIG: *Brake Judder of Cars*. In POPP, K. (editor): *Detection, Utilization and Avoidance of Nonlinear Dynamical Effects in Engineering Applications*, pages 325–352. Shaker Verlag, Aachen, 2001.
- [13] FIEGE, T.: *Reibwert- und Geräuschuntersuchungen an einer Kraftfahrzeugscheibenbremse*. Studienarbeit am Institut für Mechanik, Universität Hannover, 2000.